An engineering approach towards the design of an innovative compact photo-reactor for antibiotic removal in the frame of laboratory and pilot-plant scale

A. Almansba, A. Kane, N. Nasrallah, J.M. Wilson, R. Maachi, L. Lamaa, L. Peruchon, C. Brochier, Abdeltif Amrane, A.A. Assadi

HAL Id: hal-03335237
https://hal.science/hal-03335237

Submitted on 8 Sep 2021

An engineering approach towards the design of an innovative compact photo-reactor for antibiotic removal in the frame of laboratory and pilot-plant scale

Amira Almansba[a,b,c], Abdoulaye Kane[c], Noureddine Nasrallah[a], Jessica M. Wilson[d],

Rachida Maachi[a], Lina Lamaa[e], Laure Peruchon[e], Cedric Brochier[e], Abdeltif Amrane [b],

Aymen Amine Assadi[b*]

[a]Laboratoire de Génie de la Réaction, Faculté de Génie Mécanique et Génie des Procédés, Université des Sciences et de la Technologie Houari Boumediene, Bab Ezzouar, Alger 16111, Algérie

[b]Univ Rennes, ENSCR, CNRS, ISCR - UMR 6226, F-35000 Rennes, France

[c]UniLaSalle-Ecole des Métiers de l'Environnement, Campus de Ker Lann, 35170 Bruz, France

[d]Department of Civil and Environmental Engineering, Manhattan College 4513 Manhattan College Parkway Riverdale, NY 10463

[e]Brochier Technologies, 90 Rue Frédéric Fays, 69100 Villeurbanne Lyon, France

* **Corresponding authors:** A. Assadi, Tel.: +33(0)223238152, E-mail: <u>aymen.assadi@ensc-rennes.fr</u>

Abstract

Advanced Oxidation Processes (AOPs), in particular heterogeneous photocatalysis, have been considered as a promising method to remove antibiotics without generating hazardous intermediates. In this work, an innovative compact photoreactor was designed and tested for the degradation of the antibiotic Flumequine. The system consisted of a textile woven from both luminous and photocatalytically active fibers. The luminous fibers consisted of LED-type optical fibers and the photocatalytic fibers consist of textile fibers impregnated with TiO_2. This configuration allowed for optimization of contact between the

1

catalyst, the pollutant, and the light source. The surface morphology, elemental composition and optical properties of this photo-active fabric were characterized by SEM-EDX and by irradiance measurements. The effectiveness of the luminous textile was compared with two conventional processes: suspended TiO_2, and immobilized TiO_2 on cellulosic paper. The specific degradation rate obtained with the light textile was 28 times higher than that observed with slurry photocatalytic reactor and 65 times higher than in the case of TiO_2 supported on cellulosic paper. Luminous textile also showed efficient performance in terms of mineralization per Watt consumed with values exceeding 77 and 419 times than those obtained with suspended TiO_2 and the cellulose paper, respectively. This new configuration also improved the compactness by 3 times compared to the cellulosic paper system. The Langmuir-Hinshelwood model showed that this optical fibers-based configuration reduced the mass transfer compared to the conventional TiO_2 immobilization approaches. Additionally, the extrapolation of this process to pilot scale was successfully performed. The excellent performances in terms of degradation rate, mineralization per Watt consumed, compactness, energy consumption, and reusability make luminous textiles an attractive alternative to conventional photocatalytic reactors' design for removal of antibiotics in water and wastewater.

Keywords

1. Introduction

Since 1928, antibiotics have been used for medical treatments for both human and animal infections [1,2]. However, many of those compounds reach natural systems where they

can accumulate causing damage to both the environment and human health [3]. Additionally, their release into the environment, even at low levels, may cause resistance of microbial populations making them ineffective in the treatment of several infections [4,5]. These antibiotics are often landfilled and recalcitrant in water. To treat this water many processes have been developed, such as, adsorption, physical and chemical coagulation, biological process, and membrane filtration [6–8]. Some limitations and disadvantages associated with these treatments are: the low efficiency, the high risk of the production of harmful by-products, and the high energy consumption [9,10]. Alternatively, Advanced Oxidation Processes (AOPs), in particular heterogeneous photocatalysis, have been considered as promising alternative method [11–13] due to its ability to remove completely (mineralize) a wide range of organic pollutants at low concentrations without generating hazardous intermediates. Among the involved semiconductors, TiO_2 is one of the most currently used photocatalysts because of its high photoactivity, chemical stability and low cost [14–16]. Most studies employ TiO_2 by applying semiconductor suspensions including the high degradation and mineralization efficiency of the organic pollutants [13,17]; indeed this kind of reactor has many advantages including a very low mass transfer limitation, a possible variation of the catalyst quantity in the photoreactor, and can easily replace the photocatalyst in powders as well.

However, recovering the catalyst nanoparticles after the treatment is very challenging. To overcome the costly post-treatment, while maintaining the possibility of re-using the same catalyst for several treatment cycles, its stability and reducing the scattering that affects negatively the use of photon in slurry reactor, photocatalysts' immobilization is often considered [18–20]. However, as reported by Camera-Roda et al. [21],

there are still many shortcomings when a fixed catalyst system is implemented, including a potential low internal and external mass transfer due to a decrease of the contact between the catalyst and the pollutant. Additionally, part of the radiation can be absorbed by the support, decreasing the efficiency of the catalyst. On the other hand, the catalyst quantity in the photoreactor is restricted by the use of support, and a larger illuminated surface of the photoreactor is necessary in this type of photocatalytic system. There is a crucial disadvantage of this process, due to the use of an immersed lamp in solution as a light source inside the unit. This represents an obstacle in the design of the reactor, due to the size and the rigidity of the lamp, high energy consumption, high toxicity, and heat production [22,23].

New reactor designs with optical fibers as a support for photocatalyst have been developed and tested to overcome these problems. These reactors enhance the contact between the catalyst, the light, and the pollutant [24–26]. Various studies have been carried out to improve the photocatalytic performance of these reactors, including evaluating the influence of fiber diameter, the thickness of TiO_2, the length of the deposit on fibers, and the effect of the optical fibers number [27–30]. Although the idea of depositing the catalyst directly on the surface of the light source is interesting, there are still some drawbacks to this method associated with the attenuation of the light intensity along the axial direction of the fiber. Indeed, light intensity decreases when the fiber's length increases [31].

In this paper, we present an application of a new luminous textile manufactured by Brochier Technologies Company to remove the antibiotic Flumequine (FLU), which is an antibiotic used in veterinary medicine to treat bacterial infections. Flumequine is

commonly found in wastewater and represents a real threat to the aquatic environment [32,33].

This new textile is an innovative photocatalytic media that has not been well studied [34–36]. A particularly innovative aspect of the luminous textile lies in the simultaneous weaving of textile fibers and optical fibers, allowing the reactor to have a very compact design. Therefore, the lighted textile is considered as both a support for TiO_2 and transmitter of light through optical fibers from the source to the surface of the catalyst, combining maximization of pollutant-catalyst surface interactions with a very large illumination area of the catalyst surface (maximization of light-catalyst surface interactions). In addition, this configuration can reduce the size of the reactor over conventional reactors (miniaturization of equipment), while eliminating post-treatment and consuming less energy due to the use of LEDs (Light Emitting Diodes) as light source [37]. In this study, the potential for the luminous textile to remove FLU was compared to two conventional processes of heterogeneous photocatalysis, namely using TiO_2 in suspension and TiO_2 deposited on cellulosic paper (both systems use an immersed lamp as light source).

The results obtained were compared in terms of photocatalytic efficiencies (degradation and mineralization), energy consumption, and reactor compactness. The Langmuir-Hinshelwood model was also successfully applied to explain kinetics of the three catalytic systems studied. Here, special attention was paid to investigate the reactor compactness and the cost of FLU mg eliminated. Furthermore, a new pilot-scale photocatalytic reactor using a luminous textile with a larger size was developed in order to confirm the feasibility

of extrapolating the process to a pilot scale. The results obtained were then compared with those obtained with the lab scale.
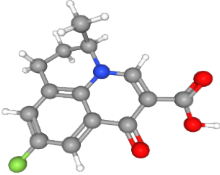
2. Material and Methods

2.1 Chemicals

Flumequine ($C_{14}H_{12}FNO_3$, ≥97.0%), (HCl, 37% v/v) and (NaOH, 98% purity) were used. All chemical reagents were purchased from sigma Aldrich supplier. Stock solutions were prepared with ultrapure water.

Physico-chemical properties of the selected pollutant and its structure are shown in Table 1.

Table 1. Physico-chemical properties and structure of the selected antibiotic.

	FLU
Chemical formula	$C_{14}H_{12}FNO_3$
MW (g mol^{-1})	261.25
λ_{max} (nm)	247
Chemical structure	

2.2 Description of the catalysts design used for photocatalysis

Photocatalytic experiments were carried out with TiO_2 catalyst in two forms: (1) powder which is TiO_2 in anatase purchased from sigma Aldrich used in a slurry configuration, and

(2) deposited on two different supports. The first was a mixture of silica, zeolite and catalyst. The catalyst is TiO_2 PC500 manufactured by Millennium company, its crystal structure is anatase (> 99%) with mean size in the range 5–10 nm. This catalyst was immobilized on non-woven cellulose fibers, provided by Ahlstrom Company (Alhström 1048). The thickness of the deposit was 250 μm. The silica (SiO_2) plays a role of an inorganic compound, it was deposited in between the cellulosic fibers and the TiO_2. The incorporation of the zeolite on the TiO_2-SiO_2 increases the adsorption capacity of the photocatalytic media (cellulosic paper) because of its large specific surface area (2000 $m^2.g^{-1}$) [38]. The detailed cellulosic paper characterization has been reported elsewhere [39,40]. Dimensions of this catalyst were $16.2.10^{-3}$ m^2 corresponding to 0.36 g of TiO_2. On the other hand, in previous studies the optimum amount of variant TiO_2 was from 0.5 up to 1 $g.L^{-1}$ for Flumequine degradation [41,42]. These two configurations (TiO_2 in powder and cellulosic paper) use a UVA lamp with a light intensity of 30 W. The second catalyst which was the luminous textile manufactured by Brochier Technologies Company (UVtex®), composed of optical fibers (in polymethyl methacrylate (PMMA) resin) and textile fibers (in polyester) woven simultaneously according to the Jacquard loom. The weft included both optical fibers and textile fibers to provide a good luminous textile strength, and the warp consisted of only optical fibers. However in the luminous textile, the light introduced is transported at the end thereof; that can be resolved by changing the light conduction properties by carrying out a specific treatment of the surface of the optical fiber, in order to allow the light to come out on its whole surface, making the textile illuminated [43]. The optical fibers had a mean diameter of 480 μm coated with 10 μm thickness of fluorinated polymer and were distributed in only one side of the luminous textile in this work, which is called the "Mono-face" (MF).

All optical fibers were assembled on one side of the textile to be connected to a cylindrical connector. The light source (LED type) was therefore directly attached to the fabric with an irradiation of the light textile of 3.1 W m^{-2}, with the emission peak centered at 365 nm.

To avoid the attack of the catalyst on the MF after its weave it was covered with Aerodisp W7622 silica and then introduced into a suspension of TiO_2-Degussa P25 to make it photocatalytically active. This operation required passage under pressure to eliminate the extra suspension; it was then dried at 70 °C for 1 h. The area of the optical fibers textile used was equal to (30x10) cm^2 and the catalyst density was 12 g_{TiO_2} .m^{-2} (corresponding to 0.36 g of TiO_2).

The luminous textile used in the pilot scale was manufactured according to the same procedure, having the same density of catalyst (12 g_{TiO_2} .m^{-2}) and using the same lamp as a light source. The difference between both textiles lay in the size, which was more important in the case of the pilot-scale; it was equal to 80x10 cm^2.

2.3   Characterization of the luminous textile

An analysis of the structural properties of the luminous textile (lab scale) was carried out by SEM-EDX (Scanning electron microscopy-energy dispersive spectroscopy X-ray diffraction) enabling both characterization of surfaces and elemental composition analysis. The optical properties of the textile were characterized by a spectrometer GL SPECTIS 1.0 UV - VIS measuring UV irradiance. The TiO_2 distribution above the luminous textile surface was evaluated by ICP-OES ACTIVA Horiba Jobin Yvon analysis (Inductively Coupled Plasma with an Optical Emission Spectrometer) on a samples of 9 cm^2 [36].

2.4   Photocatalytic experiments and photoreactor designs

In this study, two conventional configurations of photoreactors were used in lab-scale: (1) typical photocatalytic reactor with suspended photocatalyst particles; the same reactor was also adopted for tests carried out with TiO_2 immobilized on cellulosic paper, and (2) another reactor was used with luminous textile.

The major differences between these two types of design came from the light intensity and the volume of the reactor used, which were greater with the conventional photocatalytic installation. It was due to the use of an immersed light source positioned vertically in the reactor used for TiO_2 in suspension and deposited on the cellulosic paper. This light source was a UVA lamp (Phillips PL-L24 W / 10 / 4P) with a light intensity of 30 W with the emission peak centered at 365 nm; it was introduced into a sheath before immersed in solution (Fig. 1). The volume of this reactor was $1.3.10^{-3}$ m^3 (Diameter = 9.5 cm ; Height = 18 cm), and that used with the optical fiber technology was equal to 7.10^{-4} m^3 (Diameter = 5.3 cm ; Height = 38 cm) ; both were made of borosilicate glass. The intensity of the light emitted by the MF was $9.3. 10^{-2}$ W.

Each one of these reactors were filled with 600 mL of the polluted solution, which was kept under stirring (60 rpm), and recirculated using a peristaltic pump (Easy-Load Masterflex Head XX80 ELO 05) operating at a flow rate of 87 mL .mn-1 at room temperature to homogenize the solution. The pH of this solution was adjusted throughout the experiments with HCl or NaOH.

The same quantity of TiO_2 used in powder, 0.36 g, was deposited on the cellulosic paper and the MF. Before exposing the catalyst to the light, it was introduced into the solution

and kept under stirring in the dark for 1 hour in order to establish adsorption-desorption equilibrium.

At the end of each experiment carried out, the optical fiber underwent a regeneration of 90 min in water in order to be reused.
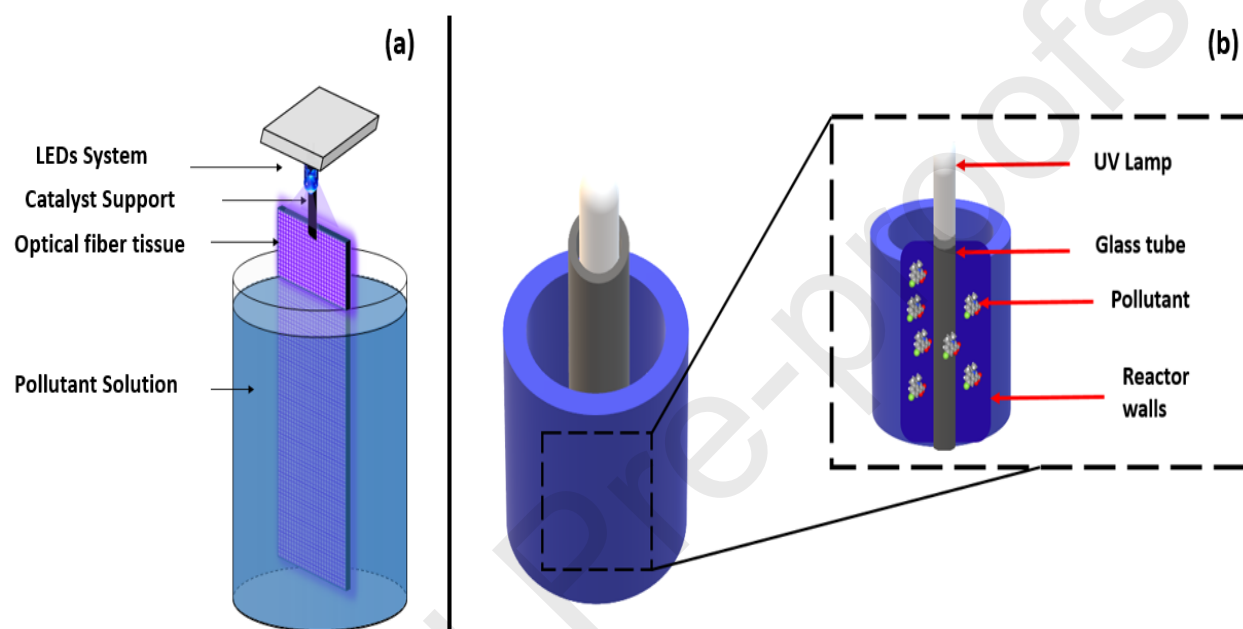

Figure. 1. Scheme of the photocatalytic set-up used for experiments on luminous textile (a) and on the suspended and immobilized systems (b).

The pilot-scale experiments were carried out in an annular recirculation reactor (Figure 2) composed of two concentric Pyrex tubes. The polluted solution was taken from a storage tank of 2 L and then recirculated after treatment using a pump (0.065 m^3 / h). The light intensity used in the pilot scale was not significantly different from the lab scale since their values were respectively equal to 3.3 W m^{-2} and 3.1 W m^{-2}. Before irradiation, the solution was submitted to an adsorption phase which lasted 60 min and after each photocatalytic experiment, the textile underwent 120 min regeneration to be reused.

The surface of the luminous textile as well as the reaction volume in the pilot scale was three times greater than in the case of the laboratory scale.
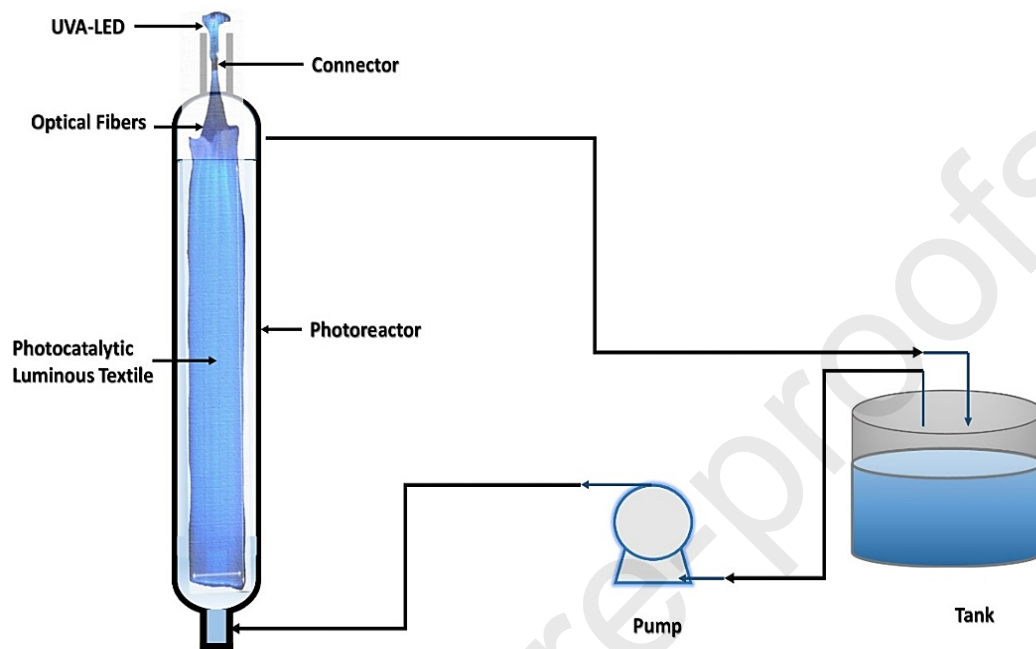

Figure 2. Scheme of the photocatalytic configuration used with pilot scale

Samples were taken over time and degradation of the FLU was tracked by measuring absorbance at 247 nm using UV-Vis spectrophotometry. The mineralization was measured by TOC-meter (Shimadzu TOC-VCSH).

Degradation efficiency (%) of FLU was determined following Equation 1,

$$\eta(\%) = \left(\frac{C_0 - C_t}{C_0}\right) x\ 100 \tag{1}$$

where C_0 and C_t are the initial pollutant concentration and the concentration at time t, respectively.

11

TOC removal was calculated following Equation 2,

$$\text{TOC removal} = \text{TOC}_0 - \text{TOC}_t \qquad\qquad (2)$$

Where TOC_0 and TOC_t are the initial Total Organic Carbon and the Total Organic Carbon at time t, respectively.

To describe and represent the kinetic mechanism of the photocatalytic process in terms of adsorption and catalysis, the Langmuir-Hinshelwood (L-H) model, which has been applied in previous similar studies [44,45], was used (Equation 3) :

$$r = -\frac{dC}{dt} = \frac{kKC}{1 + KC} \qquad\qquad (3)$$

where k (mg min^{-1} L^{-1}) is the apparent photocatalytic rate constant; K (L mg^{-1}) is the adsorption equilibrium constant, C is the initial FLU concentration (mg L^{-1}) and r is the removal rate (mg min^{-1} L^{-1}).

3. Results and discussion

3.1. Characterization of the luminous textile

3.1.1. Microscopy analysis

Figure.S1-a shows an overall view of the textile highlighting the binding points of optical fibers and textile fibers. On the sheath of the optical fibers, there were defects produced by a specific treatment, which allowed the exit of UV at its surface. Figure S1-b and S1-c also shows a deposition of a layer of TiO_2. In a previous study, it was shown that the deposition of TiO_2 is mainly focused on the surface defects of the fiber which are considered as strongly luminous zones [36].

12

The results of the chemical composition of the luminous textile are displayed in Fig. S2 ; the presence of titanium (14.34 wt.%), carbon (24.39 wt.%) and oxygen on the textile have also previously been found on cotton TiO_2 supports [46,47]. The fluorine (38.27 wt.%), on the luminous textile corresponded to the composition of the sheath of the optical fiber, which was made of fluorinated polymer. The aluminum (0.30 wt.%) was a residual compound of the surface treatment applied to the optical fiber and finally the silicon (22.33 wt.%) corresponded to the deposition of Aerodisp W7622 silica before adding the TiO_2 catalyst.

3.1.2. Irradiance measurement

To determine the distribution of light over the entire length of the textile, irradiance measurements were made on 8 different points (Fig. S3) on one side of the luminous textile before depositing the catalyst

The results obtained (Table S1) show that the textile gave a homogeneous luminous rendering over its entire surface.

In a previous study, we determined the light energy absorbed by the catalyst by measuring the irradiance of the textile before and after immobilization of TiO_2; the value obtained was equal to 3.1 W m^{-2}.

3.2. Photocatalytic performance of catalysts

Three parameters of comparison were used to compare between classical configurations (powder photocatalyst and TiO_2 deposited on cellulosic paper) and the new reactor design of photocatalysis (luminous textile) : 1) specific degradation rate, 2) reactor compactness,

and 3) mineralization. The Langmuir-Hinshelwood (L-H) model was applied for monitoring of the degradation kinetics of each system. Subsequently, experiments were performed on the MF to examine the effect of the initial concentration of the pollutant and its capacity to be reused.

3.2.1 Comparison of the photocatalytic reactor configurations

To evaluate the performance of the different photocatalytic reactor designs studied in this work three benchmarks were considered. First, the efficiency of the reactors was compared in terms of specific degradation rate (Eq. 4), expressed in mg of FLU eliminated per unit time per unit electrical power consumed. These values were determined using Eq. 3 ($-\frac{dC}{dt}$) in the beginning period of FLU degradation (for the first 20 min), then they were multiplied by the reaction volume. The values obtained were then divided by the energy consumed, which represented the light intensity emitting by the MF (9.3 10^{-2} W), and by the lamp immersed in the polluted water used in both conventional configurations of photocatalysis, TiO$_2$ in powder and cellulosic paper (30 W). Specific degradation rate was evaluated at three different initial FLU concentrations (2.5; 5 and 10 mg L^{-1}) for each configuration studied.

$$\text{Specific degradation rate} = \frac{\text{mg of FLU eliminated}}{\text{Unit time . Watt consumed}} \qquad (4)$$

The second benchmark is reactor compactness. This is important from an engineering perspective, as it is a parameter which highlights the efficiency of the reactor designs in terms of compactness as shown in Equation 5. Reactor compactness is expressed in catalytic area per unit of reactor volume. Catalytic area represents the surface of textile light and the surface of the cellulosic paper used.

14

$$\text{Reactor compactness} = \frac{\text{Catalytic area}}{\text{Reactor volume}} \qquad (5)$$

The third benchmark is mineralization performance and is expressed in TOC-removal (Eq. 2) per Watt consumed. This benchmark allows for evaluation of t FLU mineralization performance of each configuration at two initial pollutant concentrations values (5 and 20 mg L^{-1}) as shown in Equation 6.

$$\text{Mineralization performance} = \frac{\text{TOC removal}}{\text{Watt consumed}} \qquad (6)$$

For the first benchmark (specific degradation rate), as the initial concentration of the pollutant increased the specific degradation rate also increased (Figure 3). This phenomenon was observed for all tested configurations, and could be explained by more interaction between the generated of the oxidizing radicals ($^{\bullet}$OH) and pollutant molecules at the higher concentration [48]. On the other hand, as reported by Camera-Roda et al. [49] the increase in the number of pollutant molecules in the reaction medium affects the optical properties of the system and, therefore, also the absorption rate of photons and the observed reaction rate. A similar behavior has been reported by other researchers [50,51].

Figure 3 also shows that the slurry photoreactor led to higher specific degradation rates over the cellulosic paper. Indeed, most of the previous work in aqueous solution tends to indicate that the slurry system with catalyst in powder exhibit the largest photocatalytic performance as compared with equivalent loading for an immobilized system [21,52]. This could be explained by a greater contact between TiO$_2$ and the pollutant compared to the reactor with catalyst immobilized on cellulosic paper [53].

However, the most striking results was the much higher specific degradation rates observed using the MF than the conventional methods. For 10 mg L^{-1} initial FLU concentration, the rate was more than 28 times higher than that obtained with the photocatalyst reactor in suspension and almost 65 times higher than in the case of the cellulosic paper, while the energy consumption was drastically reduced.
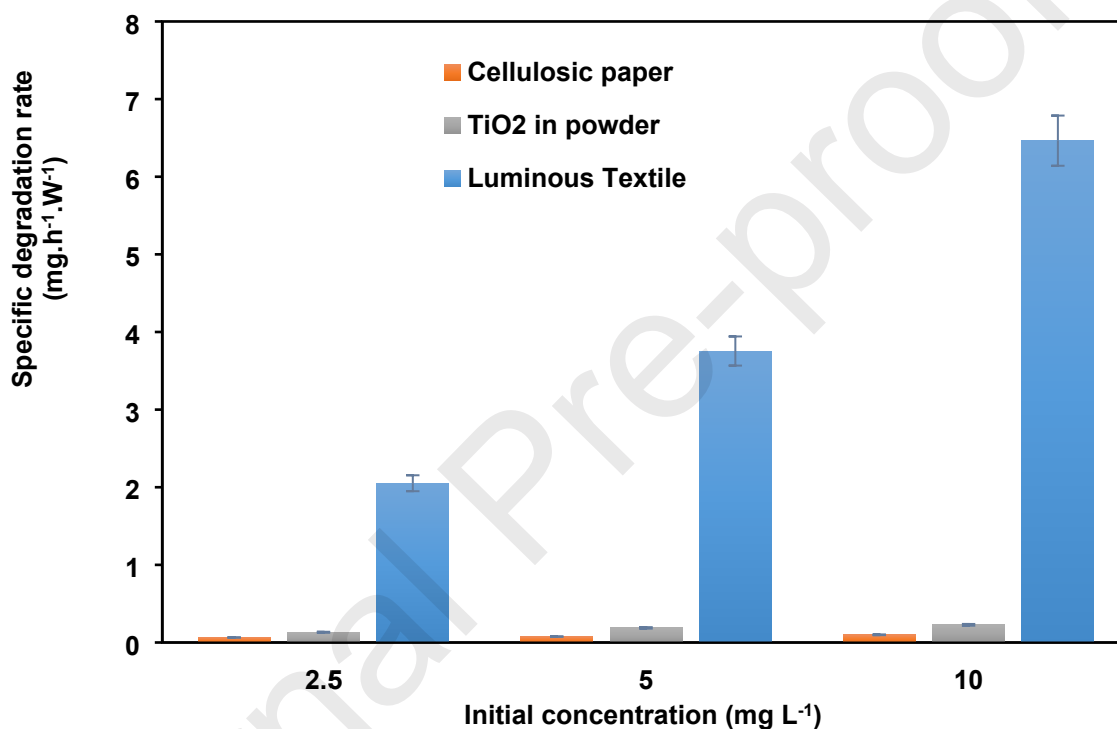

Figure. 3. Comparison of the light textile performance with conventional configurations of photocatalysis; TiO_2 amount: 0.36g; Φ (textile) =9.3 10^{-2} W; Φ (PC and TiO_2 in powder) = 30 W; C_0 (FLU) = 2.5-10 mg/L; pH ≈ 6,5; reaction volume = 600 mL; reaction time = 20 min.

The use of a support for the catalyst as well as the immersed lamp inside the unit as a light source takes up reactor space and requires a larger illuminated surface of the catalyst as argued by Camera-Roda et al [21]. Using luminous textile allows a better reactor compactness than the conventional immobilized system via cellulosic paper, because of

the integration of the light source with the catalytic support. As shown in figure 4, this configuration improved the compactness by 3 times compared to the cellulosic paper system.
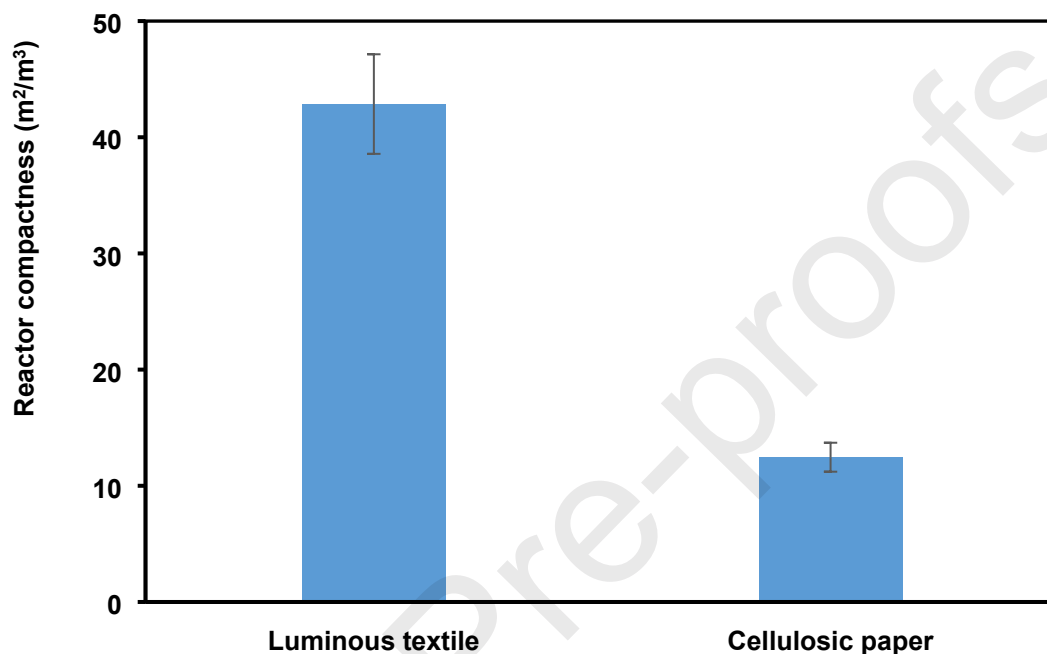

Figure. 4. Comparison of luminous textile with conventional immobilized system, in terms of reactor compactness.

Similarly, the MF was clearly more efficient in terms of TOC-removal per watt consumed, with values reaching 419 times greater than obtained with cellulosic paper system and almost 77 times greater than with suspended TiO_2 (Fig. 5). The performance of MF could be explained by the optimization of the contact between the catalyst and the light source [35]. Figure 5 also shows that the mineralization efficiency decreased when the pollutant concentration increased from 5 to 20 mg L^{-1}; this could be explained by the increase in the number of pollutant molecules, while the catalyst quantity remained unchanged [54].
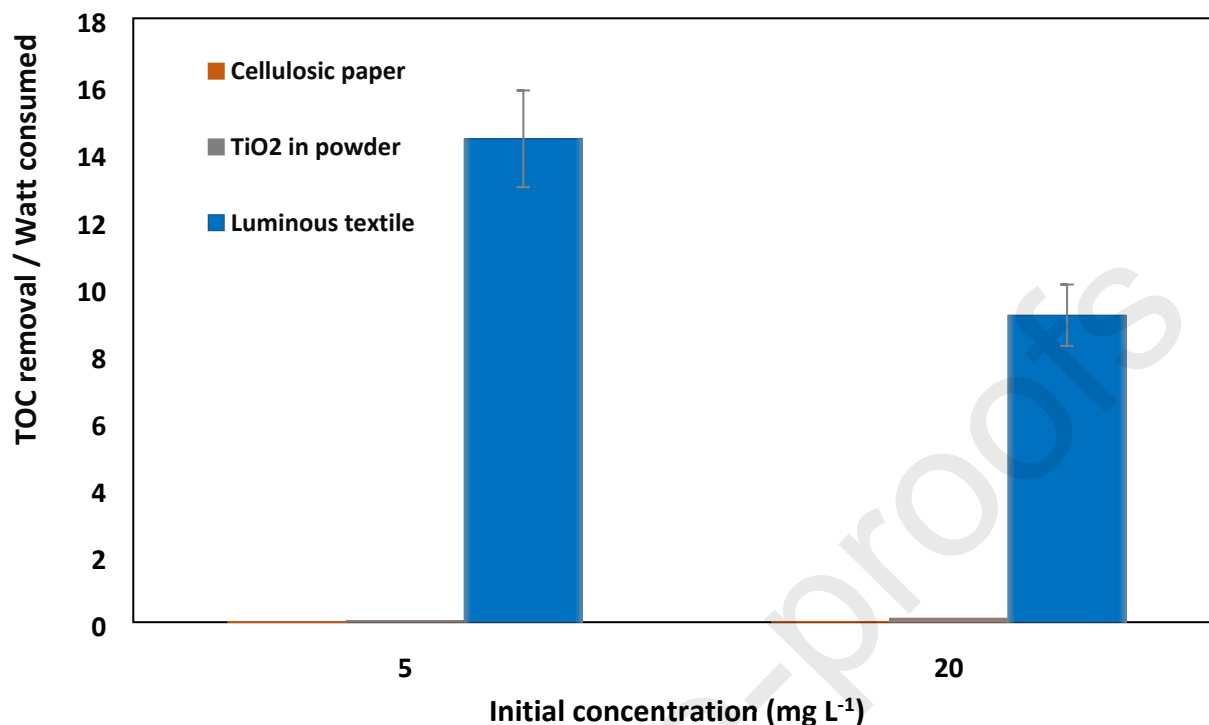
17

Figure. 5. Comparison of luminous textile with conventional configurations of photocatalysis, in terms of TOC-removal / Watt consumed; TiO_2 amount: 0.36g ; Φ (textile) =9.3 10^{-2} W ; Φ (PC and TiO_2 in powder) = 30 W; C_0 (FLU) = 5 and 20 mg/L ; pH ≈ 6,5 ; Reaction volume = 600 mL; reaction time = 195 min.

3.2.1.1 Kinetic mechanism of FLU degradation

It is essential to understand and identify the kinetic mechanism of degradation for photocatalytic reactions. For this purpose, the Langmuir-Hinshelwood model (Eq 3) was used to assess the performances of the catalysts studied for FLU removal. This model has been widely used for modeling experimental data for the degradation kinetics of various organic pollutants [55,56].

After rearrangement and linearization of Eq. 3 ($r = \frac{kKC}{1+KC}$), the L-H model is shown in Equation 7 The inverse of the initial degradation rate ($\frac{1}{r0}$) as a function of the inverse of the initial pollutant concentration ($\frac{1}{C0}$) was plotted (Figure 6).

$$\frac{1}{r} = \frac{1}{kKC} + \frac{1}{k} \qquad (7)$$

For each configuration 4 experiments at different initial FLU concentration (2.5 mg L^{-1}; 5 mg L^{-1}; 10 mg L^{-1} and 20 mg L^{-1}) were performed. The initial degradation rate, r_0, was calculated using Eq. 3 ($-\frac{dC}{dt}$) for the first 20 min of each experiment. R^2 (regression coefficient) values revealed that the L-H model was in good agreement with the experimental results obtained; it was also shown that the initial degradation rate was inversely affected by the increasing of initial FLU concentration (Fig. 6).

The k (apparent rate constant) obtained using TiO$_2$ in suspension (k = 0.22 mg L^{-1} min^{-1}) was higher than the corresponding values reported for the luminous textile (k = 0.13 mg L^{-1} min^{-1}) and the cellulosic paper (k = 0.10 mg L^{-1} min^{-1}). Previous research has shown that the slurry photocatalytic reactor provides much better contact between catalyst and pollutant compared to immobilized systems because of better dispersion of the catalyst particles in the liquid phase [57–59]. However, the use of the catalyst in suspension presents important drawbacks as previously discussed. Alternatively, the degradation rate constant of the luminous textile was higher than that obtained with cellulosic paper, most likely due to enhanced mass transfer process, thus improving the photocatalytic performances compared to conventional immobilized systems [34].
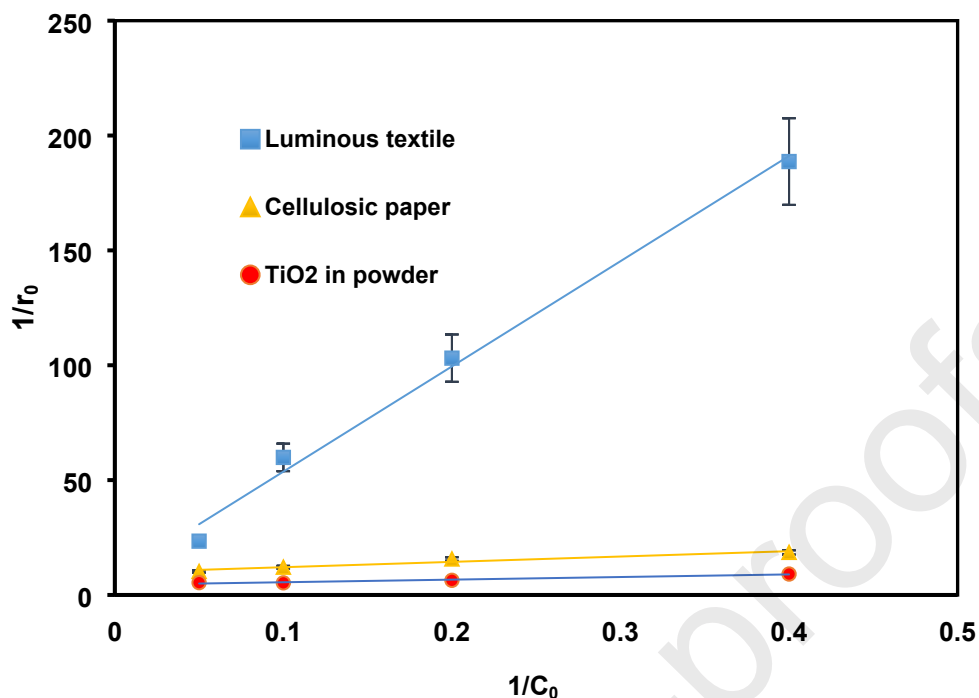
Figure. 6. Linearized Langmuir-Hinshelwood plot for photocatalytic FLU removal using Luminous textile (■), Cellulosic paper (▲) and TiO_2 in suspension (●) at pH = 6.5; $[FLU]_o$ = 2.5-20 mg L^{-1}; reaction solution = 600 mL; reaction time = 20 min.

The results of the apparent rate constant obtained with the MF were compared with studies previously carried out by Lou et al. [47] with an immobilized catalyst system. Table 2 shows that the k obtained with the textile was 2 times lower. However, the light intensity used was almost 4 times higher in the case of the immobilized system reported by Lou et al. This confirms the great potential of the light textile regarding the energy economy.

Table. 2. Comparison of the apparent rate constant values of the L-H model and the energy consumed for luminous textile and immobilized TiO_2 previously reported in the literature

20

	UV intensity (W m^{-2})	k (mg L^{-1} min^{-1})
Luminous textile (This study)	3.13	0.13
Lou et al., 2017 [60]	12	0.28

3.2.2 Impact of the operating parameters on the performances of the luminous textile

3.2.2.1 Effect of the initial FLU concentration

The effect of the initial concentration on the degradation and mineralization of the pollutant was examined for 2.5, 5, 10, and 20 ppm of FLU, with the MF as a catalyst. Photolysis experiments were also carried out using a virgin optical fiber (which did not contain catalyst). For each condition, the reaction time was 330 min, while the other conditions were kept constant (TOC / TOC$_0$ ratios were determined after 330 min).

As shown in Figure 7, a very low degradation rate was obtained using the virgin optical fiber, even after 330 min irradiation.

On the other hand, the highest degradation efficiency and mineralization yields obtained with luminous textile impregnated with TiO$_2$ were 87% and 57%, respectively for an initial FLU concentration equal to 2.5 mg. L^{-1}.

Fig. 7 also shows a decrease in the efficiency of degradation and mineralization by increasing the initial FLU concentration. This could be explained by the saturation of the active sites present on the catalyst surface. In fact, the number of radical species remains unchanged by maintaining the same quantity of TiO$_2$, while the number of pollutant

molecules in the reaction medium increases with its initial amount. Consequently, the elimination efficiency of the substrate decreases [60,61].
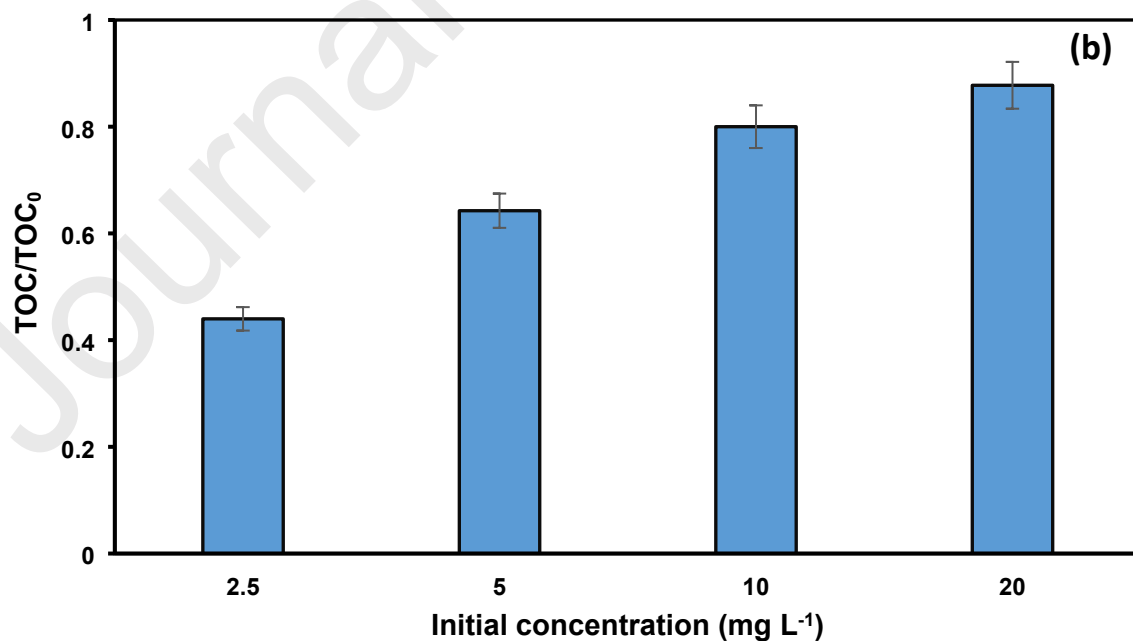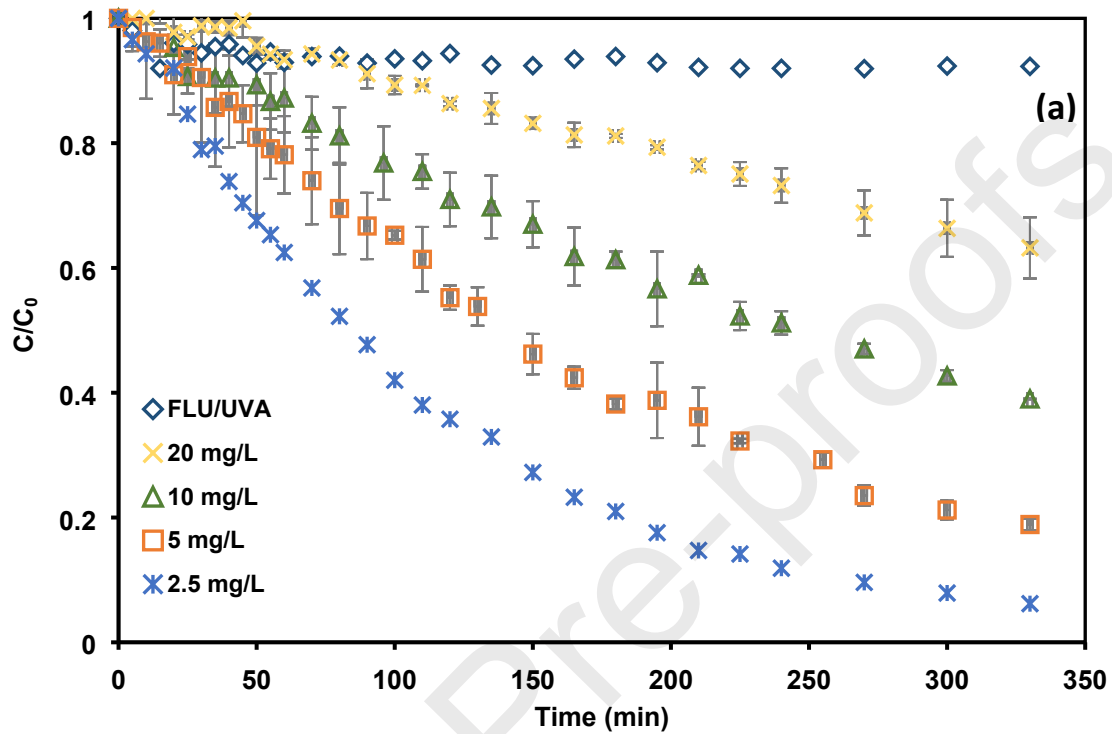
Figure. 7. Time profiles of C/C_0 for FLU degradation (a) TOC/TOC_0 versus initial concentration of FLU (b) with luminous textile configuration at pH = 6.5; $[FLU]_o$ = 2.5-20 mg L^{-1}; reaction solution = 600 mL; reaction time = 330 min.

Table 3 summarizes some reported works related to TiO_2-based photocatalysts used for wastewater treatment containing pharmaceutical compounds. As can be seen in the table 4, the luminous textile shows a very satisfying degradation rate, while consuming a lower light intensity compared to other studies, and has also the advantage to eliminate the post-treatment. Adding to this it improves the photoreactors compactness due to the integration of light source in the photocatalytic support.

Table 3. Summary of TiO_2-based photocatalysts for pharmaceutical compounds photodegradation.

Pollutant	Photocatalyst	Light source (nm)	Irradiation time (min)	Degradation (%)	Light intensity	Ref.
4-chlorophenol	Immobilized CNT-TiO_2 layer	365	300	70	10 W/m^2	[62]
2,4-dichloropheno-xyacetic (2,4-D)	Fe_2O_3-TiO_2	365	240	48.64	6 W	[63]

23

Ibuprofen	Aeroxide P25	350-400	121	62	9W	[64]
Flumequine	Luminous textile	365	330	87	$9.3.10^{-2}$	In this work

3.2.2.2 Reusability of the luminous textile

The recyclability of the catalyst is an important factor from both environmental and economic points of view [40]. To examine this parameter, the luminous textile underwent two cycles of photocatalysis under the same operating conditions (Figure 8). k_{app} was calculated after 210 min of irradiation with reference to Eq. 8; the values obtained were almost identical for the two cycles, 0.0029 min^{-1} and 0.0027 min^{-1}, respectively. Between these two cycles, six experiments were carried out and each of them was followed by 90 minutes of regeneration operation. All of these experiments represent 1450 consecutive minutes of photocatalytic operation of the light textile. We have obtained a similar reproducibility efficiency for more longer treatment durations in a previous work [65]. This observation highlighted the great stability of the catalyst, even after long periods of running, which can be attributed to the absence of deposit or accumulation on the catalytic surface. Therefore, the generation of radical species responsible for the degradation was not affected during the photocatalytic experiments.

$$\text{Ln}\left(\frac{C_t}{C_0}\right) = - kapp \cdot t \qquad\qquad (8)$$

Where k_{app} is the apparent kinetic constant and t is the reaction time (min)

24

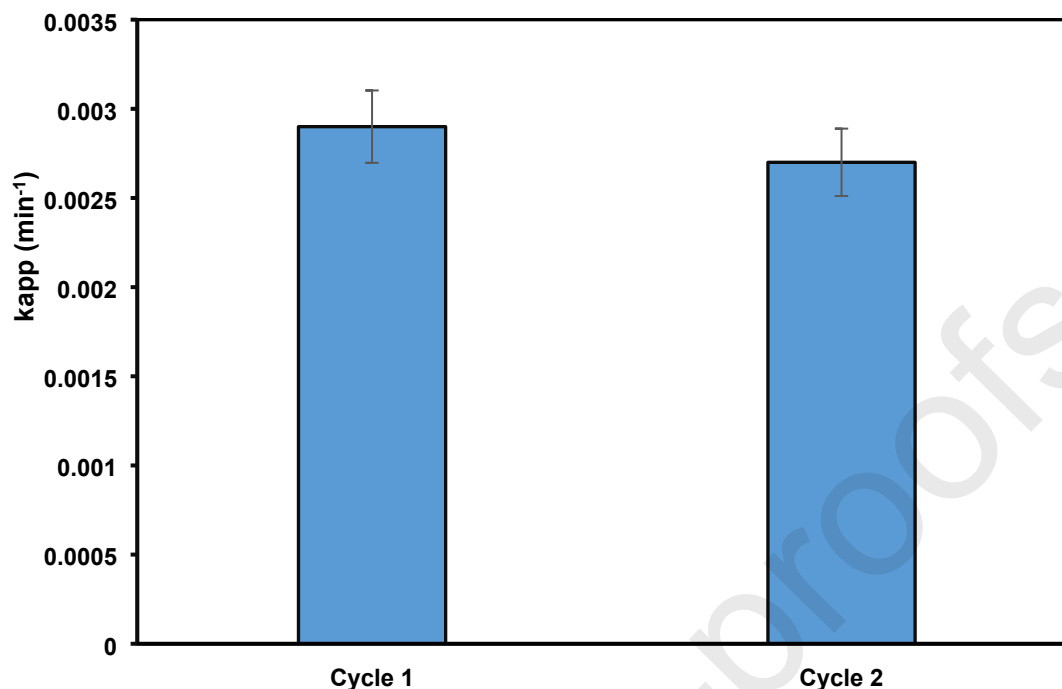**Figure. 8**. Reusability cycles of the luminous textile at pH 3, $[FLU]_o$ = 10 mg L^{-1}, reaction solution = 600 mL; reaction time = 210 min.

3.2.3 Study in a pilot-scale reactor

The performance of the luminous textile was tested in a recirculating annular reactor in an attempt to provide evidence of its potential to scale up to industrial conditions. The effect of the initial concentration in the range from 2.5 to 10 mg L^{-1} was examined.

Figure 9 shows that the efficiency decreased by increasing the initial FLU concentration. This could be explained by the saturation of the active sites present on the catalyst surface. This is similar to the concentration effects observed previously (see 3.3.1), as the number of radical species remains unchanged by maintaining the same quantity of TiO_2, while the number of pollutant molecules in the reaction medium increases with its initial amount [66].

The maximum degradation was achieved for 2.5 mg L^{-1} of FLU, reaching 75% after 330 min.
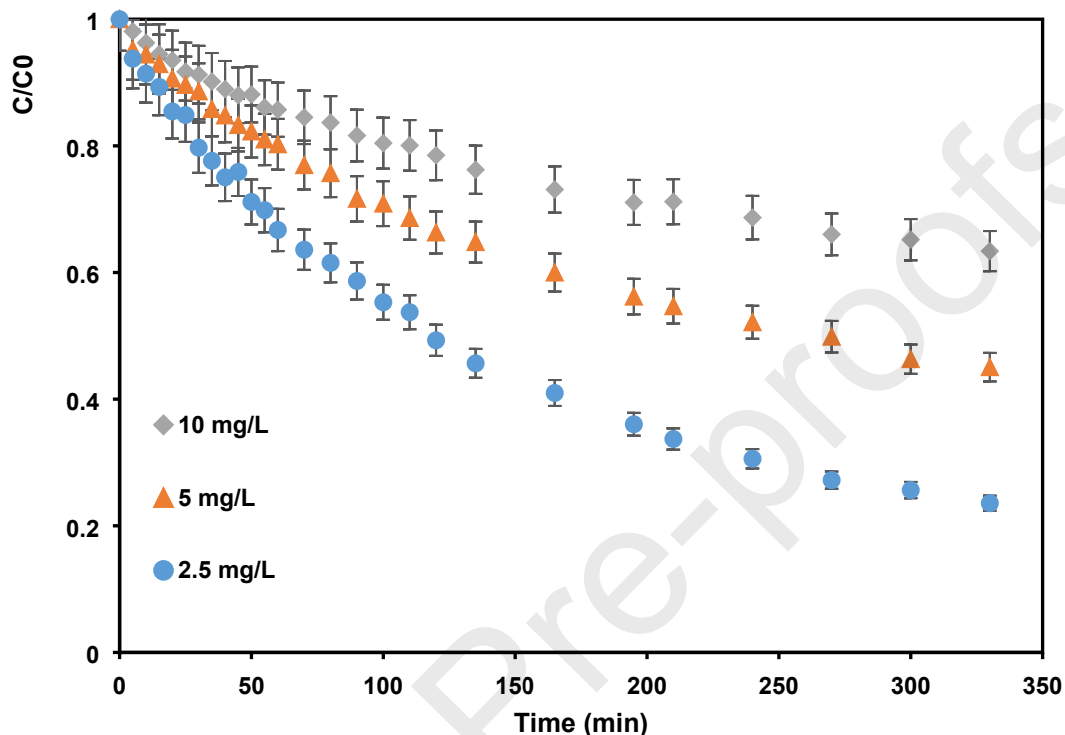

Figure. 9. Time profiles of C/C$_0$ for FLU degradation with luminous textile at pH = 6.5; [FLU]o = 2.5-10 mg L^{-1}; reaction solution = 2000 mL; reaction time = 330 min.

3.2.4 Comparative study between the pilot scale and the laboratory scale

To evaluate the performance of the light textile on a larger scale, the specific degradation rates as well as the constants of the L-H model obtained with both pilot-scale and lab scale were compared. These two systems operating at recirculation flow rates that are respectively equal to 0.065 m³/h and 5.10^{-3} m³/h. Figure 10 summarizes the main differences between the laboratory scale and the pilot scale. This figure shows that for

almost the same light intensity the volume of the solution treated by the textile at the pilot

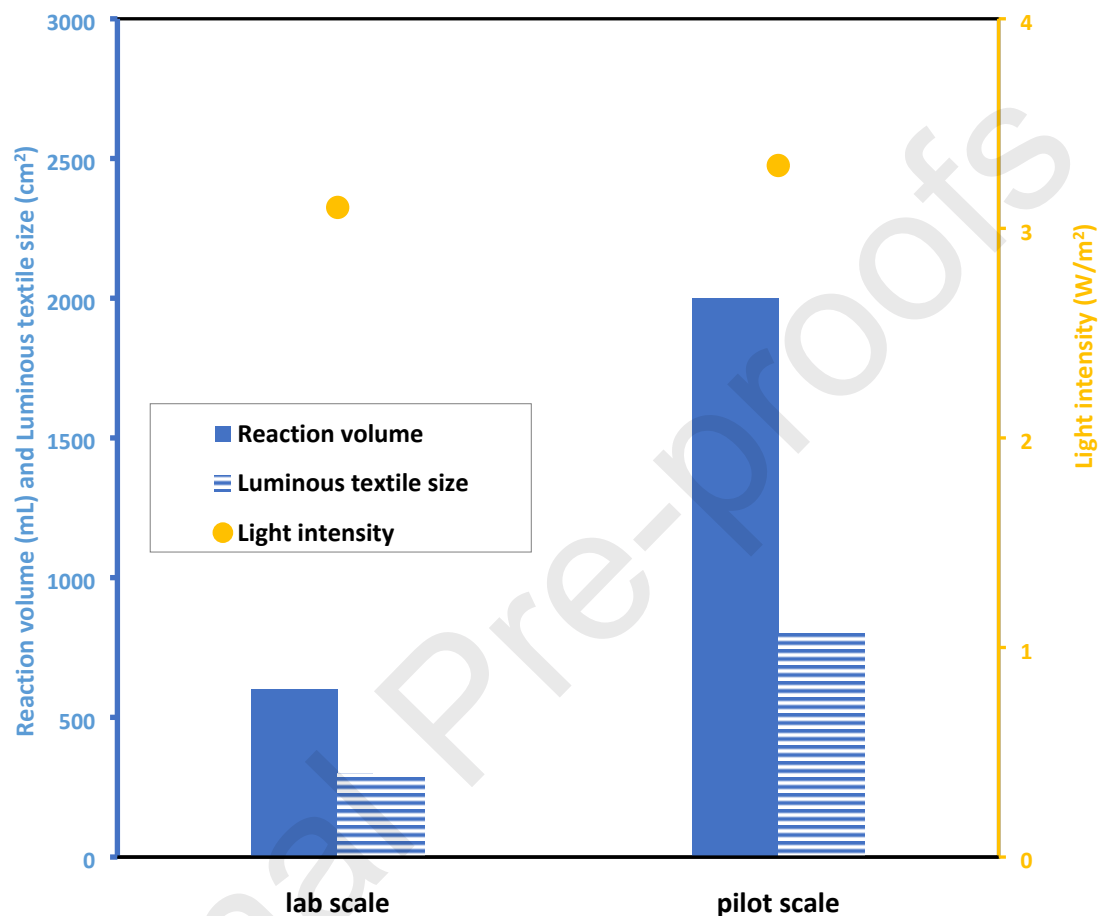scale is three times greater than that treated at the laboratory scale.

Figure. 10. Differences between the laboratory scale and the pilot scale.

3.2.4.1 Comparison in terms of specific degradation rate

The specific degradation rates at the pilot scale were calculated using Eq. 4 at different

initial FLU concentrations (2.5; 5 and 10 mg L^{-1}), the results obtained were then compared

with those of the lab scale (Fig. 11).

27

As seen in Figure 11, the specific degradation rates obtained with the pilot scale are higher than those obtained with the laboratory scale. This could be explained by the increase in the recirculation flow rate of the polluted solution in the case of the pilot scale. Based on the research of Malekshoar et al. [57], at low fluid flow rates when an immobilized catalyst system is implemented the accessibility of the catalytic surface to the photons and the pollutant is reduced. The laminar thin film formed around the particles of the catalyst became thinner by enhancing the mixing intensity. Therefore, the contact between the photocatalyst and molecules of pollutant is increased and consequently the overall reaction rate increases.
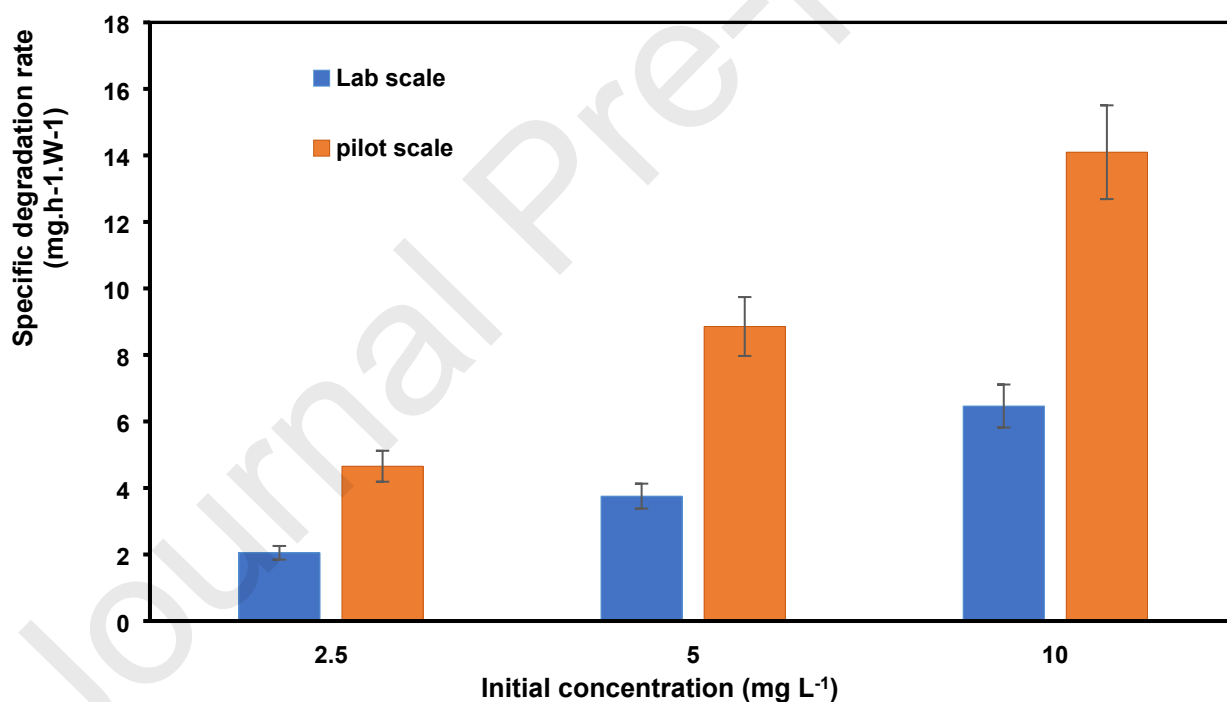

Figure. 11 Comparison between the pilot scale and the laboratory scale in terms of specific degradation rate; C_0 (FLU) = 2.5-10 mg/L; pH ≈ 6,5; reaction time = 20 min.

3.2.4.2 Comparison of kinetic mechanisms

The results obtained at the pilot-scale were modeled using the linearized Langmuir-Hinshelwood equation to gain a better understanding of the photocatalytic process and to compare its performances with those obtained on the laboratory scale.

Figure 6 demonstrated that $\frac{1}{r0}$ versus $\frac{1}{C0}$ showed good linearity with R^2 = 0.997. L–H model constants were calculated and listed in the Table 4 for both pilot-scale and lab scale.

Table 4. Langmuir-Hinshelwood model constants at pilot-scale and laboratory scale.

	Lab scale	Pilot scale
k (mg L^{-1} min^{-1})	0.13	0.11
K (L mg^{-1})	0.02	0.04

Table. 4 shows that the values of k_{pilot} and k_{lab} were very close, showing that the luminous textile retained its performances at scale greater than that of the laboratory while using an identical light intensity.

This first series of experiments describes the feasibility of the process at a pilot scale while consuming very little energy and providing valuable perspectives to extrapolate the process to a larger scale.

4. Conclusion

In the present work, experiments of Flumequine photodegradation using luminous textile were performed. Such configuration represents a new design of a compact photocatalytic reactor serving as both support for the catalyst and conveyor of UV light to its surface.

The performance of the luminous textile was compared with two conventional photocatalytic processes including slurry TiO_2 and catalyst immobilized on cellulose paper with a lamp immersed in the reactor as a light source. The parameters for comparison between these three reactor designs were: specific degradation rate, mineralization per watt consumed, reactor compactness and apparent constant rate obtained by the Langmuir-Hinshelwood model. It was observed that the luminous textile exhibited the highest values of specific degradation rate and mineralization per watt consumed due to an optimized contact between the catalyst and the light source on the one hand and the low energy consumption due to use of LEDs, which are energy efficient, on the other hand. Higher performances were also noted for the luminous textile in terms of compactness because of the integration of the light source in the catalytic support. The textile also showed a higher apparent rate constant than that obtained with the immobilized classical system due to an enhanced contact between the light and the particles of catalyst. These results showed that optical fibers technology represents a gain in energy, compactness and photocatalytic efficiency for the elimination of flumequine compared to conventional systems, while keeping good reuse capacity. Furthermore, this study also showed the feasibility of extrapolating the process to a pilot scale in an attempt to approach industrial conditions.

Acknowledgments

References:

[1]   A. Jia, Y. Wan, Y. Xiao, J. Hu, Occurrence and fate of quinolone and fluoroquinolone antibiotics in a municipal sewage treatment plant, Water Research. 46 (2012) 387–394. https://doi.org/10.1016/j.watres.2011.10.055.

[2]   Y. Xiang, X. Yang, Z. Xu, W. Hu, Y. Zhou, Z. Wan, Y. Yang, Y. Wei, J. Yang, D.C.W. Tsang, Fabrication of sustainable manganese ferrite modified biochar from vinasse for enhanced adsorption of fluoroquinolone antibiotics: Effects and mechanisms, Science of The Total Environment. 709 (2020) 136079. https://doi.org/10.1016/j.scitotenv.2019.136079.

[3]   H. Huang, S. Zeng, X. Dong, D. Li, Y. Zhang, M. He, P. Du, Diverse and abundant antibiotics and antibiotic resistance genes in an urban water system, Journal of Environmental Management. 231 (2019) 494–503. https://doi.org/10.1016/j.jenvman.2018.10.051.

[4]   A. Laffite, P.I. Kilunga, J.M. Kayembe, N. Devarajan, C.K. Mulaji, G. Giuliani, V.I. Slaveykova, J. Poté, Hospital Effluents Are One of Several Sources of Metal, Antibiotic Resistance Genes, and Bacterial Markers Disseminated in Sub-Saharan Urban Rivers, Front. Microbiol. 7 (2016). https://doi.org/10.3389/fmicb.2016.01128.

[5]   K. Uchida, Y. Konishi, K. Harada, M. Okihashi, T. Yamaguchi, M.H.N. Do, L. Thi Bui, T. Duc Nguyen, P. Do Nguyen, D. Thi Khong, H. Thi Tran, T. Nam Nguyen, H. Viet Le, V. Van Chau, K. Thi Van Dao, H. Thi Ngoc Nguyen, K. Kajimura, Y. Kumeda, K. Tran Pham, K. Ngoc Pham, C. Trong Bui, M. Quang Vien, N. Hoang Le, C. Van Dang, K. Hirata, Y. Yamamoto, Monitoring of Antibiotic Residues in Aquatic Products in Urban and Rural Areas of Vietnam, J Agric Food Chem. 64 (2016) 6133–6138. https://doi.org/10.1021/acs.jafc.6b00091.

[6]   K. Zare, V.K. Gupta, O. Moradi, A.S.H. Makhlouf, M. Sillanpää, M.N. Nadagouda, H. Sadegh, R. Shahryari-ghoshekandi, A. Pal, Z. Wang, I. Tyagi, M. Kazemi, A comparative study on the basis of adsorption capacity between CNTs and activated carbon as adsorbents for removal of noxious synthetic dyes: a review, J Nanostruct Chem. 5 (2015) 227–236. https://doi.org/10.1007/s40097-015-0158-x.

[7]   T. Singh, N. Srivastava, P.K. Mishra, A.K. Bhatiya, N.L. Singh, Application of TiO_2 Nanoparticle in Photocatalytic Degradation of Organic Pollutants, MSF. 855 (2016) 20–32. https://doi.org/10.4028/www.scientific.net/MSF.855.20.

[8]   F. Yu, Y. Li, S. Han, J. Ma, Adsorptive removal of antibiotics from aqueous solution using carbon materials, Chemosphere. 153 (2016) 365–385. https://doi.org/10.1016/j.chemosphere.2016.03.083.

[9]   M. de Kwaadsteniet, P.H. Dobrowsky, A. van Deventer, W. Khan, T.E. Cloete, Domestic Rainwater Harvesting: Microbial and Chemical Water Quality and Point-of-Use Treatment Systems, Water Air Soil Pollut. 224 (2013) 1629. https://doi.org/10.1007/s11270-013-1629-7.

[10] I. Béchohra, A. Couvert, A. Amrane, Absorption and biodegradation of toluene: Optimization of its initial concentration and the biodegradable non-aqueous phase liquid volume fraction, International Biodeterioration & Biodegradation. 104 (2015) 350–355. https://doi.org/10.1016/j.ibiod.2015.07.004.

[11] R. Liang, J.C. Van Leuwen, L.M. Bragg, M.J. Arlos, L.C.M. Li Chun Fong, O.M. Schneider, I. Jaciw-Zurakowsky, A. Fattahi, S. Rathod, P. Peng, M.R. Servos, Y.N. Zhou, Utilizing UV-LED pulse width modulation on TiO2 advanced oxidation processes to enhance the decomposition efficiency of pharmaceutical micropollutants, Chemical Engineering Journal. 361 (2019) 439–449. https://doi.org/10.1016/j.cej.2018.12.065.

[12] A. Patchaiyappan, S. Saran, S.P. Devipriya, Recovery and reuse of TiO2 photocatalyst from aqueous suspension using plant based coagulant - A green approach, Korean J. Chem. Eng. 33 (2016) 2107–2113. https://doi.org/10.1007/s11814-016-0059-9.

[13] A. Carabin, P. Drogui, D. Robert, Photo-degradation of carbamazepine using TiO2 suspended photocatalysts, Journal of the Taiwan Institute of Chemical Engineers. 54 (2015) 109–117. https://doi.org/10.1016/j.jtice.2015.03.006.

[14] N.H. Ahmad Barudin, S. Sreekantan, M.T. Ong, C.W. Lai, Synthesis, characterization and comparative study of nano-Ag–TiO2 against Gram-positive and Gram-negative bacteria under fluorescent light, Food Control. 46 (2014) 480–487. https://doi.org/10.1016/j.foodcont.2014.05.046.

[15] M. Nasr, C. Eid, R. Habchi, P. Miele, M. Bechelany, Recent Progress on Titanium Dioxide Nanomaterials for Photocatalytic Applications, ChemSusChem. 11 (2018) 3023–3047. https://doi.org/10.1002/cssc.201800874.

[16] P. Nyamukamba, O. Okoh, H. Mungondori, R. Taziwa, S. Zinya, Synthetic Methods for Titanium Dioxide Nanoparticles: A Review, in: D. Yang (Ed.), Titanium Dioxide - Material for a Sustainable Environment, InTech, 2018. https://doi.org/10.5772/intechopen.75425.

[17] G. Ghasemzadeh, M. Momenpour, F. Omidi, M.R. Hosseini, M. Ahani, A. Barzegari, Applications of nanomaterials in water treatment and environmental remediation, Frontiers of Environmental Science & Engineering. 8 (2014) 471–482. https://doi.org/10.1007/s11783-014-0654-0.

[18] M.J. Torralvo, J. Sanz, I. Sobrados, J. Soria, C. Garlisi, G. Palmisano, S. Çetinkaya, S. Yurdakal, V. Augugliaro, Anatase photocatalyst with supported low crystalline TiO2: The influence of amorphous phase on the activity, Applied Catalysis B: Environmental. 221 (2018) 140–151. https://doi.org/10.1016/j.apcatb.2017.08.089.

[19] M.E. Leblebici, G.D. Stefanidis, T. Van Gerven, Comparison of photocatalytic space-time yields of 12 reactor designs for wastewater treatment, Chemical Engineering and Processing: Process Intensification. 97 (2015) 106–111. https://doi.org/10.1016/j.cep.2015.09.009.

[20] R. van Grieken, J. Marugán, C. Sordo, C. Pablos, Comparison of the photocatalytic disinfection of E. coli suspensions in slurry, wall and fixed-bed reactors, Catalysis Today. 144 (2009) 48–54. https://doi.org/10.1016/j.cattod.2008.11.017.

[21] G. Camera Roda, V. Loddo, L. Palmisano, F. Parrino, Chapter 6 - Special Needs and Characteristic Features of (Photo)catalytic Reactors with a Review of the Proposed Solutions, in: G. Marcì, L. Palmisano (Eds.), Heterogeneous Photocatalysis, Elsevier, 2019: pp. 177–213. https://doi.org/10.1016/B978-0-444-64015-4.00006-7.

[22] F. Khodadadian, A. Poursaeidesfahani, Z. Li, J.R. van Ommen, A.I. Stankiewicz, R. Lakerveld, Model-Based Optimization of a Photocatalytic Reactor with Light-Emitting Diodes, Chemical Engineering & Technology. 39 (2016) 1946–1954. https://doi.org/10.1002/ceat.201600010.

[23] W.-K. Jo, R.J. Tayade, New Generation Energy-Efficient Light Source for Photocatalysis: LEDs for Environmental Applications, Ind. Eng. Chem. Res. 53 (2014) 2073–2084. https://doi.org/10.1021/ie404176g.

[24] K. Hofstadler, Rupert. Bauer, S. Novalic, G. Heisler, New Reactor Design for Photocatalytic Wastewater Treatment with TiO2 Immobilized on Fused-Silica Glass Fibers: Photomineralization of 4-Chlorophenol, Environ. Sci. Technol. 28 (1994) 670–674. https://doi.org/10.1021/es00053a021.

[25] W. Choi, J.Y. Ko, H. Park, J.S. Chung, Investigation on TiO2-coated optical fibers for gas-phase photocatalytic oxidation of acetone, Applied Catalysis B: Environmental. 31 (2001) 209–220. https://doi.org/10.1016/S0926-3373(00)00281-2.

[26] H. Joo, H. Jeong, M. Jeon, I. Moon, The use of plastic optical fibers in photocatalysis of trichloroethylene, Solar Energy Materials and Solar Cells. 79 (2003) 93–101. https://doi.org/10.1016/S0927-0248(02)00372-0.

[27] A. Danion, J. Disdier, C. Guillard, F. Abdelmalek, N. Jaffrezic-Renault, Characterization and study of a single-TiO2-coated optical fiber reactor, Applied Catalysis B: Environmental. 52 (2004) 213–223. https://doi.org/10.1016/j.apcatb.2004.04.005.

[28] A. Danion, C. Bordes, J. Disdier, J.-Y. Gauvrit, C. Guillard, P. Lantéri, N. Jaffrezic-Renault, Optimization of a single TiO2-coated optical fiber reactor using experimental design, Journal of Photochemistry and Photobiology A: Chemistry. 168 (2004) 161–167. https://doi.org/10.1016/j.jphotochem.2004.03.002.

[29] A. Danion, J. Disdier, C. Guillard, O. Païssé, N. Jaffrezic-Renault, Photocatalytic degradation of imidazolinone fungicide in TiO2-coated optical fiber reactor, Applied Catalysis B: Environmental. 62 (2006) 274–281. https://doi.org/10.1016/j.apcatb.2005.08.008.

[30] A. Danion, J. Disdier, C. Guillard, N. Jaffrezic-Renault, Malic acid photocatalytic degradation using a TiO2-coated optical fiber reactor, Journal of Photochemistry and Photobiology A: Chemistry. 190 (2007) 135–140. https://doi.org/10.1016/j.jphotochem.2007.03.022.

[31] R.-D. Sun, A. Nakajima, I. Watanabe, T. Watanabe, K. Hashimoto, TiO2-coated optical fiber bundles used as a photocatalytic filter for decomposition of gaseous organic compounds, Journal of Photochemistry and Photobiology A: Chemistry. 136 (2000) 111–116. https://doi.org/10.1016/S1010-6030(00)00330-0.

[32] M. Feng, L. Yan, X. Zhang, P. Sun, S. Yang, L. Wang, Z. Wang, Fast removal of the antibiotic flumequine from aqueous solution by ozonation: Influencing factors, reaction pathways, and toxicity evaluation, Science of The Total Environment. 541 (2016) 167–175. https://doi.org/10.1016/j.scitotenv.2015.09.048.

[33] A. Labella, M. Gennari, V. Ghidini, I. Trento, A. Manfrin, J.J. Borrego, M.M. Lleo, High incidence of antibiotic multi-resistant bacteria in coastal areas dedicated to fish farming, Mar. Pollut. Bull. 70 (2013) 197–203. https://doi.org/10.1016/j.marpolbul.2013.02.037.

[34] P.-A. Bourgeois, E. Puzenat, L. Peruchon, F. Simonet, D. Chevalier, E. Deflin, C. Brochier, C. Guillard, Characterization of a new photocatalytic textile for formaldehyde removal from indoor air, Applied Catalysis B: Environmental. 128 (2012) 171–178. https://doi.org/10.1016/j.apcatb.2012.03.033.

[35] C. Indermühle, E. Puzenat, F. Simonet, L. Peruchon, C. Brochier, C. Guillard, Modelling of UV optical ageing of optical fibre fabric coated with TiO2, Applied Catalysis B: Environmental. 182 (2016) 229–235. https://doi.org/10.1016/j.apcatb.2015.09.037.

[36] C. Indermühle, E. Puzenat, F. Dappozze, F. Simonet, L. Lamaa, L. Peruchon, C. Brochier, C. Guillard, Photocatalytic activity of titania deposited on luminous textiles for water treatment, Journal of Photochemistry and Photobiology A: Chemistry. 361 (2018) 67–75. https://doi.org/10.1016/j.jphotochem.2018.04.047.

[37] B.M. da Costa Filho, A.L.P. Araujo, S.P. Padrão, R.A.R. Boaventura, M.M. Dias, J.C.B. Lopes, V.J.P. Vilar, Effect of catalyst coated surface, illumination mechanism and light source in heterogeneous TiO2 photocatalysis using a mili-photoreactor for n-decane oxidation at gas phase, Chemical Engineering Journal. 366 (2019) 560–568. https://doi.org/10.1016/j.cej.2019.02.122.

[38] A.A. Assadi, A. Bouzaza, D. Wolbert, P. Petit, Isovaleraldehyde elimination by UV/TiO2 photocatalysis: comparative study of the process at different reactors configurations and scales, Environ Sci Pollut Res Int. 21 (2014) 11178–11188. https://doi.org/10.1007/s11356-014-2603-7.

[39] A. Rabahi, A.A. Assadi, N. Nasrallah, A. Bouzaza, R. Maachi, D. Wolbert, Photocatalytic treatment of petroleum industry wastewater using recirculating annular reactor: comparison of experimental and modeling, Environ Sci Pollut Res. 26 (2019) 19035–19046. https://doi.org/10.1007/s11356-018-2954-6.

[40] G.N. Coulibaly, S. Rtimi, A.A. Assadi, K. Hanna, Nano-sized iron oxides supported on polyester textile to remove fluoroquinolones in hospital wastewater, Environmental Science.Nano. 7 (2020) 2156. https://doi.org/10.1039/d0en00261e.
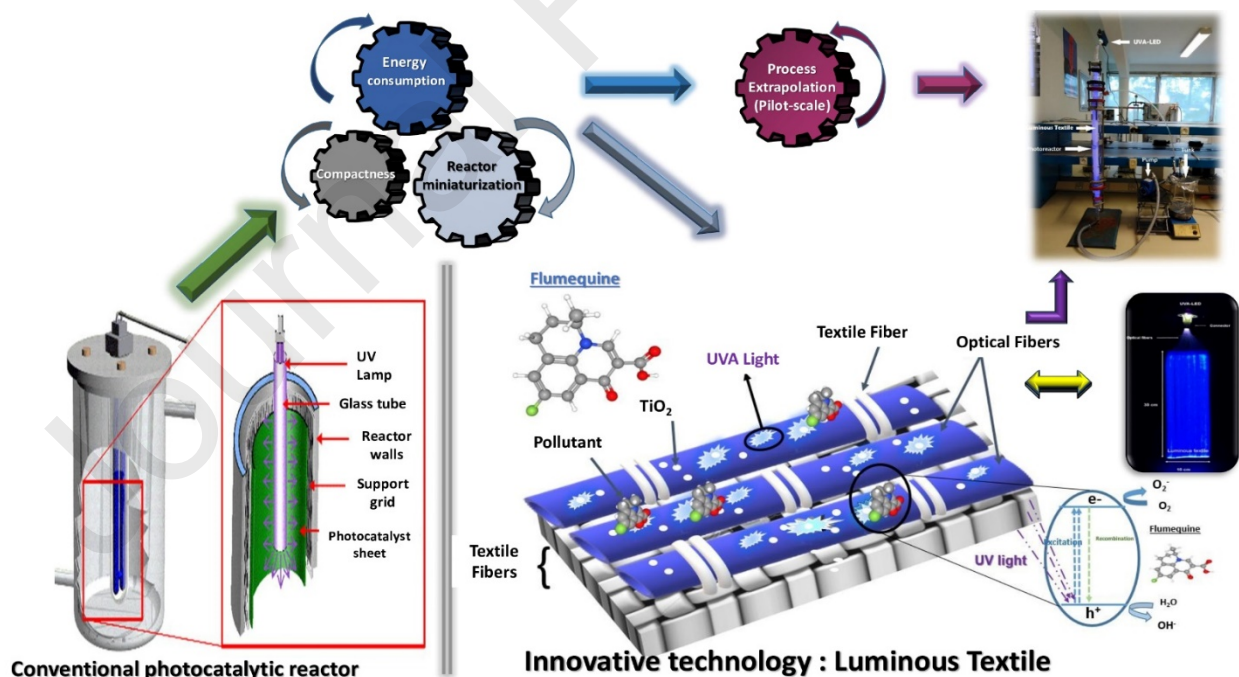
[41] R. Palominos, J. Freer, M.A. Mondaca, H.D. Mansilla, Evidence for hole participation during the photocatalytic oxidation of the antibiotic flumequine, Journal of Photochemistry and Photobiology A: Chemistry. 193 (2008) 139–145. https://doi.org/10.1016/j.jphotochem.2007.06.017.

[42] A.A. Assadi, J. Palau, A Bouzaza, D Wolbert, Modeling of a continuous photocatalytic reactor for isovaleraldehyde oxidation: effect of different operating parameters and chemical degradation pathway, Chemical Engineering Research and Design 91 (2013), 1307-1316.

[43] C. BROCHIER, E. DEFLIN, T. BRETING, ILLUMINATING COMPLEX - ALSTOM TRANSPORT SA, WO 2008/062141, 2008. http://www.sumobrain.com/patents/wipo/Illuminating-complex/WO2008061789.html (accessed September 8, 2019).

[44] N.G. Asenjo, R. Santamaría, C. Blanco, M. Granda, P. Álvarez, R. Menéndez, Correct use of the Langmuir–Hinshelwood equation for proving the absence of a synergy effect in the photocatalytic degradation of phenol on a suspended mixture of titania and activated carbon, Carbon. 55 (2013) 62–69. https://doi.org/10.1016/j.carbon.2012.12.010.

[45] Computational modelling of a photocatalytic UV-LED reactor with internal mass and photon transfer consideration, Chemical Engineering Journal. 264 (2015) 962–970. https://doi.org/10.1016/j.cej.2014.12.013.

[46] W.A. Daoud, J.H. Xin, Y.-H. Zhang, Surface functionalization of cellulose fibers with titanium dioxide nanoparticles and their combined bactericidal activities, Surface Science. 599 (2005) 69–75. https://doi.org/10.1016/j.susc.2005.09.038.

[47] M.J. Uddin, F. Cesano, F. Bonino, S. Bordiga, G. Spoto, D. Scarano, A. Zecchina, Photoactive TiO2 films on cellulose fibres: synthesis and characterization, Journal of Photochemistry and Photobiology A: Chemistry. 189 (2007) 286–294. https://doi.org/10.1016/j.jphotochem.2007.02.015.

[48] G. Camera-Roda, V. Augugliaro, A.G. Cardillo, V. Loddo, L. Palmisano, F. Parrino, F. Santarelli, A reaction engineering approach to kinetic analysis of photocatalytic reactions in slurry systems, Catalysis Today. 259 (2016) 87–96. https://doi.org/10.1016/j.cattod.2015.05.007.

[49] G. Camera-Roda, V. Loddo, L. Palmisano, F. Parrino, Guidelines for the assessment of the rate law of slurry photocatalytic reactions, Catalysis Today. 281 (2017) 221–230. https://doi.org/10.1016/j.cattod.2016.06.050.

[50] A. Hassani, A. Khataee, S. Karaca, M. Fathinia, Heterogeneous photocatalytic ozonation of ciprofloxacin using synthesized titanium dioxide nanoparticles on a montmorillonite support: parametric studies, mechanistic analysis and intermediates identification, RSC Adv. 6 (2016) 87569–87583. https://doi.org/10.1039/C6RA19191F.

[51] R.R. Solís, I.F. Mena, M.N. Nadagouda, D.D. Dionysiou, Adsorptive interaction of peroxymonosulfate with graphene and catalytic assessment via non-radical pathway for the removal of aqueous pharmaceuticals, Journal of Hazardous Materials. 384 (2020) 121340. https://doi.org/10.1016/j.jhazmat.2019.121340.

[52] A.E. Cassano, O.M. Alfano, Reaction engineering of suspended solid heterogeneous photocatalytic reactors, Catalysis Today. 58 (2000) 167–197. https://doi.org/10.1016/S0920-5861(00)00251-0.

[53] M. Delnavaz, B. Ayati, H. Ganjidoust, S. Sanjabi, Application of concrete surfaces as novel substrate for immobilization of TiO2 nano powder in photocatalytic treatment of phenolic water, J Environ Health Sci Engineer. 13 (2015) 58. https://doi.org/10.1186/s40201-015-0214-y.

[54] H. Hassena, Photocatalytic Degradation of Methylene Blue by Using Al2O3/Fe2O3 Nano Composite under Visible Light, Mod Chem Appl. (2016). https://doi.org/10.4172/2329-6798.1000176.

[55] H. Lin, H. Zhang, X. Wang, L. Wang, J. Wu, Electro-Fenton removal of Orange II in a divided cell: Reaction mechanism, degradation pathway and toxicity evolution, Separation and Purification Technology. 122 (2014) 533–540. https://doi.org/10.1016/j.seppur.2013.12.010.

[56] P. Pascariu, M. Homocianu, C. Cojocaru, P. Samoila, A. Airinei, M. Suchea, Preparation of La doped ZnO ceramic nanostructures by electrospinning–calcination method: Effect of La3+ doping on optical and photocatalytic properties, Applied Surface Science. 476 (2019) 16–27. https://doi.org/10.1016/j.apsusc.2019.01.077.

[57] G. Malekshoar, A.K. Ray, In-situ grown molybdenum sulfide on TiO2 for dye-sensitized solar photocatalytic hydrogen generation, Chemical Engineering Science. 152 (2016) 35–44. https://doi.org/10.1016/j.ces.2016.05.029.

[58] A.A. Assadi, A. Bouzaza, D. Wolbert, Study of synergetic effect by surface discharge plasma/TiO2 combination for indoor air treatment: Sequential and continuous configurations at pilot scale, Journal of Photochemistry and Photobiology A: Chemistry. 310 (2015) 148–154. https://doi.org/10.1016/j.jphotochem.2015.05.007.

[59] M.E. Leblebici, J. Rongé, J.A. Martens, G.D. Stefanidis, T. Van Gerven, Computational modelling of a photocatalytic UV-LED reactor with internal mass and photon transfer consideration, Chemical Engineering Journal. 264 (2015) 962–970. https://doi.org/10.1016/j.cej.2014.12.013.

[60] W. Lou, A. Kane, D. Wolbert, S. Rtimi, A.A. Assadi, Study of a photocatalytic process for removal of antibiotics from wastewater in a falling film photoreactor: Scavenger study and process intensification feasibility, Chemical Engineering and Processing: Process Intensification. 122 (2017) 213–221. https://doi.org/10.1016/j.cep.2017.10.010.

[61] H. Zeghioud, M. Kamagate, L.S. Coulibaly, S. Rtimi, A.A. Assadi, Photocatalytic degradation of binary and ternary mixtures of antibiotics: reactive species investigation in pilot scale, Chemical Engineering Research and Design. 144 (2019) 300–309. https://doi.org/10.1016/j.cherd.2019.02.015.

[62] R. Zouzelka, Y. Kusumawati, M. Remzova, J. Rathousky, T. Pauporté, Photocatalytic activity of porous multiwalled carbon nanotube-TiO2 composite layers for pollutant degradation,

Journal of Hazardous Materials. 317 (2016) 52–59. https://doi.org/10.1016/j.jhazmat.2016.05.056.

[63] M. Kamagate, A.A. Assadi, T. Kone, S. Giraudet, L. Coulibaly, K. Hanna, Use of laterite as a sustainable catalyst for removal of fluoroquinolone antibiotics from contaminated water Chemosphere 195 (2018) 847-853.

[64] A.A. Assadi, S. Loganathan, P.N. Tri, S. Gharib-Abou Ghaida, A. Bouzaza, A. N. Tuan, D. Wolbert, Pilot scale degradation of mono and multi volatile organic compounds by surface discharge plasma/TiO2 reactor: Investigation of competition and synergism, Journal of hazardous materials 357 (2018) 305-313.

[65] A. Almansba, A. Kane, N. Nasrallah, R. Maachi, L. Lamaa, L. Peruchon, C. Brochier, I. Béchohra, A. Amrane, A.A. Assadi, Innovative photocatalytic luminous textiles optimized towards water treatment: Performance evaluation of photoreactors, Chemical Engineering Journal. 416 (2021) 129195. https://doi.org/10.1016/j.cej.2021.129195.

[66] M. Dou, J. Wang, B. Gao, C. Xu, F. Yang, Photocatalytic difference of amoxicillin and cefotaxime under visible light by mesoporous g-C3N4: Mechanism, degradation pathway and DFT calculation, Chemical Engineering Journal. 383 (2020) 123134. https://doi.org/10.1016/j.cej.2019.123134.

Graphical abstract

Conventional photocatalytic reactor

Innovative technology : Luminous Textile

- Antibiotic was treated using a TiO2 deposed on new configuration of luminous textile.

- The luminous textile represents a gain in energy, compactness and photocatalytic efficiency.

- Kinetics removal were well modeling with using L-H model.

- The feasibility of process extrapolating to a pilot scale was verified.